THE JOURNAL OF BIOLOGICAL CHEMISTRY VOL. 281, NO. 47, pp. 36082–36090, November 24, 2006

Kindlin-1 Is a Phosphoprotein Involved in Regulation of Polarity, Proliferation, and Motility of Epidermal Keratinocytes*

Received for publication, June 29, 2006, and in revised form, August 15, 2006 Published, JBC Papers in Press, October 1, 2006, DOI 10.1074/jbc.M606259200

Corinna Herz[‡§], Monique Aumailley[¶‖], Carsten Schulte[¶], Ursula Schlötzer-Schrehardt[**], Leena Bruckner-Tuderman[‡], and Cristina Has[‡1]

*From the [‡]Department of Dermatology, University Medical Center Freiburg, Hauptstrasse 7, 79104 Freiburg, Germany, [§]Institute of Biology, University of Freiburg, Schänzlestrasse 1, 79104 Freiburg, Germany, [¶]Center for Biochemistry, University of Cologne, Joseph-Stelzmann-strasse 52, 50931 Cologne, Germany, [‖]Center for Molecular Medicine Cologne, University of Cologne, Joseph-Stelzmann-strasse 52, 50931 Cologne, Germany, and the **Department of Ophthalmology, University of Erlangen, Schwabachanlage 6, 91054 Erlangen, Germany*

A novel family of focal adhesion proteins, the kindlins, is involved in attachment of the actin cytoskeleton to the plasma membrane and in integrin-mediated cellular processes. Deficiency of kindlin-1, as a result of loss-of-function mutations in the *KIND1* gene, causes Kindler syndrome, an autosomal recessive genodermatosis characterized by skin blistering, progressive skin atrophy, photosensitivity and, occasionally, carcinogenesis. Here we characterized authentic and recombinantly expressed kindlin-1 and show that it is localized in basal epidermal keratinocytes in a polar fashion, close to the cell surface facing the basement membrane, in the areas between the hemidesmosomes. We identified two forms of kindlin-1 in keratinocytes, with apparent molecular masses of 78 and 74 kDa, corresponding to phosphorylated and desphosphorylated forms of the protein. In kindlin-1-deficient skin, basal keratinocytes show multiple abnormalities: cell polarity is lost, proliferation is strongly reduced, and several cells undergo apoptosis. *In vitro*, deficiency of kindlin-1 in keratinocytes leads to strongly reduced cell proliferation, decreased adhesion, undirected motility, and intense protrusion activity of the plasma membrane. Taken together, these results show that kindlin-1 plays a role in keratinocyte adhesion, polarization, proliferation, and migration. It is involved in organization and anchorage of the actin cytoskeleton to integrin-associated signaling platforms.

The Kindler syndrome protein, kindlin-1, is a member of a newly described protein family, which also includes kindlin-2 (also known as pleckstrin homology domain containing family C member 1 or mitogen-inducible gene 2 protein, Mig-2) and kindlin-3 (also known as Unc-112-related protein 2). The family members show a high amino acid sequence homology to each other and to the *Caenorhabditis elegans* protein UNC-112 (1). The homology to UNC-112 has led to functional predictions about the kindlins as linkers of the cytoskeleton to the plasma membrane (1). *C. elegans* embryos homozygous for *unc-112* null mutations exhibit a Pat (paralyzed arrested elongation at 2-fold) terminal phenotype, *i.e.* they arrest at the 2-fold stage of embryogenesis and have severely disorganized body wall muscle. Correspondingly, UNC-112-GFP fusion protein was localized to dense bodies and M-lines, structures that attach the myofilament lattice to the muscle cell membrane (2).

The functional predictions are supported by the fact that all three kindlins contain a FERM[2] domain (band four-point-one/ezrin/radixin/moesin), interrupted by a pleckstrin homology (PH) domain. The 298-amino acid FERM domain was originally identified in band 4.1 isolated from human erythrocyte ghosts. FERM proteins provide a regulated linkage from filamentous actin in the cortex to membrane proteins on the surface of cells. Their conformation and activity are regulated by a combination of phospholipid binding and phosphorylation and seems to play a crucial role in the cellular cytoskeletal response to Rho pathway activation (3). PH domains share little sequence conservation but all have an electrostatically polarized common fold. PH domains have diverse functions including targeting proteins to the plasma membrane and strong specificity for lipid binding. They are present in protein kinases, guanine nucleotide exchange factors, and GTPase-activating proteins for small GTP-binding proteins and phospholipases (4).

Kindlin-2 or Mig-2 was shown to be a component of the cell-extracellular matrix adhesion structures in keratinocytes (5). Small interfering RNA-mediated gene silencing demonstrated that Mig-2 is indispensable for proper control of cell shape change (6). Yeast two-hybrid screens suggested that Mig-2 interacts with a novel protein, migfilin, a widely expressed component of the actin-cytoskeleton-membrane junctions, which play key roles in cell shape modulation, motility, and differentiation (5).

* This work was supported in part by a grant from Research Commission of the Medical Faculty of the University of Freiburg and the ROSA Skin Research Award (to C. H.), by the Network Epidermolysis bullosa grant from the Federal Ministry for Education and Research (BMBF), projects 5 and 9, and by ZMMK Grant TV80 (to M. A.). The costs of publication of this article were defrayed in part by the payment of page charges. This article must therefore be hereby marked "*advertisement*" in accordance with 18 U.S.C. Section 1734 solely to indicate this fact.

[1] To whom correspondence should be addressed. Tel.: 49-761-270-6785; Fax: 49-761-270-6720; E-mail: crishas@haut.ukl.uni-freiburg.de.

[2] The abbreviations used are: FERM, four-point-one/ezrin/radixin/moesin; PH, pleckstrin homology; KS, Kindler syndrome; NHK, normal human keratinocytes; CK2, casein kinase II; TBB, 4,5,6,7-tetrabromo-2-azabenzimidazole; IIF, indirect immunofluorescence; DEJZ, dermal-epidermal junction zone; MAPK, mitogen-activated protein kinase; TBS, Tris-buffered saline; TUNEL, terminal deoxynucleotidyltransferase-mediated dUTP nick end labeling.

The above observations are in line with the first studies showing co-localization of kindlin-1-GFP fusion protein with the actin cytoskeleton and also with vinculin, a component of focal contacts (1, 7). In the epidermis kindlin-1 was found in basal keratinocytes, predominantly in the cytoplasma (1). In HaCaT epithelial cells, kindlin-1 expression was inducible by transforming growth factor-β, the protein formed a complex with the cytoplasmic domain of β1 integrin, and reduction of kindlin-1 expression by small interfering RNA perturbed cell spreading (7).

Indirect genetic evidence for kindlin-1 functions is provided by Kindler syndrome (KS), a human disorder, characterized by skin blistering at birth and in early childhood, mucosal fragility, progressive poikiloderma, mild photosensitivity, and, occasionally, carcinogenesis (8). Identification of null mutations in the kindlin-1 gene, *KIND1*, in patients with KS permitted both molecular diagnosis of the disease and structural predictions of the *KIND1* gene product, kindlin-1 (1, 9). However, very little is known about biochemical characteristics and physiological functions of kindlin-1 or the phenotypic consequences of its alterations in KS.

Here we used biochemical, functional, and genetic studies to characterize authentic kindlin-1 in human skin and cultivated primary keratinocytes. We show that it has two physiological forms, phosphorylated and dephosphorylated, and that it is intimately involved in the regulation of cell shape, adhesion, polarity, proliferation, and motility.

EXPERIMENTAL PROCEDURES

Recombinant Protein Expression and Antibody Production—Two glutathione *S*-transferase expression constructs spanning the C-terminal part of kindlin-1 were engineered (Fig. 1*A*). To obtain the shorter kindlin-1 fragment (spanning amino acids 620–674), a 165-bp PCR product was generated from cDNA obtained from normal human keratinocyte (NHK) total RNA using the forward primer KS2F: 5′-GCGCGGATCCCAGGTGGTCATCGAGTTTGA-3′, the reverse primer KS1R: 5′-GCGCGAATTCGCCGGTCAATTTGTGGAA-3′. For the larger fragment (spanning amino acids 541–674), a 402-bp amplicon was generated using the forward primer KS1F: 5′-GCGCGGATCCCAGAACGTGGCCCAGATG-3′ and the reverse primer KS1R. Both PCR fragments were cloned into BamHI and EcoRI sites of the p-GEX-6P-1 vector (Amersham Biosciences), verified by DNA sequencing and then used to transform BL21 cells (Amersham Biosciences). The insoluble recombinant proteins trapped in inclusion bodies were loaded onto SDS-PAGE, briefly stained with BioSafe Coomassie Blue (Bio-Rad), and excised from the gel. Gel pieces containing the kindlin-1 fragments were used for immunization of rabbits with standard immunization protocols (Eurogentec). The antisera were affinity-purified with recombinant kindlin-1 immobilized to nitrocellulose. After washing of the membranes with TBS, the antibodies were eluted with 0.1 M glycine (pH 2.5) and neutralized immediately with 1 M unbuffered Tris. A third antibody was produced in rabbits against a polypeptide spanning amino acids 153–171 of kindlin-1 (Fig. 1*A*) and affinity purified (PANATecs).

Protein Extraction and Immunoblotting—Different cell types were lysed in a buffer containing 1% Nonidet P-40, 20 mM Tris-Cl (pH 7.5), 100 mM NaCl, 4 mM EDTA, and 1 mM Pefabloc for 30 min at 4 °C. The lysates were centrifuged at 14,000 rpm for 30 min at 4 °C; and the supernatants were transferred into clean tubes and assayed for protein concentration with the DC protein assay (Bio-Rad). The samples were heated for 3 min at 90 °C in blue sample buffer containing 0.1 M dithiothreitol, separated by 10% SDS-PAGE, and transferred onto nitrocellulose. The blots were incubated with primary antibodies overnight at 4 °C, followed by incubation with alkaline phosphatase-linked anti-rabbit or anti-mouse IgG (Sigma) or horseradish peroxidase-labeled anti-mouse IgG (Bio-Rad). Primary antibodies against following proteins were used: kindlin-1 (affinity-purified), tubulin (Sigma), MAPK diphosphorylated ERK-1 and -2 (Sigma), His-G (Invitrogen), vinculin (Chemicon), talin (Sigma), ILK (Upstate Biotechnology), keratin 5 (Dako), and β1 integrin (Chemicon). Visualization was with nitro blue tetrazolium and 5-bromo-4-chloro-3-indolyl phosphate in detection buffer or with ECL Plus system (Amersham Biosciences).

Assays for Cell Proliferation, Adhesion, Migration, and Apoptosis—Human keratinocytes from normal or KS skin and HaCaT cells were cultivated in keratinocyte growth medium (Invitrogen) and COS-7 cells in Dulbecco's modified Eagle's medium (Invitrogen) with 10% fetal calf serum and 1% glutamate. Normal human foreskin melanocytes were obtained from PromoCell. Cell morphology and shape were observed and photographed with the phase-contrast digital compact camera C-7070 (Olympus). Proliferation assays were performed in duplicates, as described (10). Cell adhesion assays were performed in triplicates on 96-well plates coated with 10 μg/ml of fibronectin or 2 μg/ml of laminin 332. The wells were blocked with 1% bovine serum albumin for 1 h. Equal amounts of NHK and KS keratinocytes (10^4 cells) were plated for 1 h, washed, trypsinized, and counted (10, 11).

The *in vitro* wound closure assay was performed as described (11), with modifications. Keratinocytes were seeded on 6-well plates coated with laminin 332 in duplicates and grown to 90% confluence. Then the cell monolayers were scratched with a pipette tip. Three scratches for NHK and KS keratinocytes were photographed with a digital compact camera C-7070 (Olympus) immediately after wounding and then every 2 h during 12 h. The wound area was measured using the program ImageJ version1.37g (rsb.info.nih.gov/ij/).

Keratinocyte migration was monitored with time-lapse video microscopy and image analysis. The cells were seeded in keratinocyte growth medium, and after reaching 40–50% confluence, cell movements were recorded in a chamber (37 °C, 5% CO_2) placed on an inverted microscope (Axiovert S100TV, Zeiss) equipped with a digital CCD camera (Xillix MicroImager). Phase contrast photographs were automatically captured every 5 min for 3 h and stored with the Open lab software system (Improvision). The image sequences were converted to Quick Time movies, and migration tracks and cell shape changes were analyzed using Dynamic Image Analysis System software (Solltech Inc.). Cell velocity (μm/min) and direction of migration were calculated from the trajectories of at least 40 cells for each population. Shape changes of single cells were

determined by measuring in successive frames (12 frames, 1 frame/5 min) the areas involved in protrusion and retraction of the plasma membrane.

Apoptosis in cell cultures was assessed with the M30-Apoptosense ELISA kit (PEVIVA) (Alexis).

cDNA Synthesis and Transfection Studies—Total RNA was extracted with QiAmp RNA blood mini kit (Qiagen) from subconfluent NHK. Reverse transcription was performed with Advantage RT-for-PCR Kit (BD Biosciences) with 0.5 μg of total RNA, using oligo(dT) primers. For amplification of full-length *KIND1* cDNA, the oligonucleotides: 5′-ATGCTGTCATCCACTGACTT-3′ (forward) and 5′-GAGACAGATCAGCACGAGGA-3′ (reverse) were used. The PCR reaction was performed in a 50-μl volume containing 200 ng of cDNA, 1× buffer 2 with 2.5 mM Mg^{2+}, 0.2 mM dNTP, 0.5 μM of each primer, and 2.5 units of the Expand High Fidelity PCR System (Roche Diagnostics). The cycling conditions were as follows: denaturation at 94 °C for 2 min, followed by 30 cycles of 94 °C for 30 s, 56 °C for 30 s, and extension at 70 °C for 2 min 30 s; final extension was for 10 min at 70 °C. The PCR product was cloned into the vector pcDNA4/HisMax using the TOPOTA expression kit (Invitrogen). The construct was verified by DNA sequencing and used for transfection of subconfluent COS-7 and HaCaT cells with 150 ng *KIND1* cDNA per cm^2 and the Lipofectamine 2000 reagent (Invitrogen).

Immunostainings and Confocal Microscopy—Skin cryosections were blocked with 0.1% bovine serum albumin/TBS for 30 min. The specimen were stained with primary antibodies against kindlin-1, integrins α3 (P1B5, Chemicon), and α6 (GoH3, kindly provided by Dr. A. Sonnenberg, The Netherlands Cancer Institute, Amsterdam), collagen XVII (12, 13), Ki67 (Dako), keratins 5 and 10 (Dako), and involucrin (Sigma). As secondary antibodies, FITC-, rhodamine-, or Cy3-labeled anti-mouse or anti-rabbit IgG or the AEC system (Dako) were used. The signals were visualized with confocal laser scanning microscopy (LSM510, Carl Zeiss) or light microscopy. 4′,6-Diamidino-2-phenylindole was used as nuclear stain and hematoxylin as counter stain. The TUNEL assay was performed with the DeadEnd Colorimetric System (Promega), as recommended by the manufacturer.

Immunoelectron Microscopy—For post-embedding immunogold labeling, tissue specimens were fixed in 4% paraformaldehyde and 0.1% glutaraldehyde in 0.1 M cacodylate buffer (pH 7.4) for 2–5 h at 4 °C. Specimens were dehydrated serially to 70% ethanol at −20 °C and embedded in LR White resin. Ultrathin sections were successively incubated in TBS, 0.05 M glycine in TBS, 0.5% ovalbumin, and 0.5% fish gelatin in TBS, primary antibody diluted in TBS-ovalbumin overnight at 4 °C, and, finally, 10 nm gold-conjugated secondary antibody (BioCell) diluted 1:30 in TBS-ovalbumin for 1 h. After rinsing, the sections were stained with uranyl acetate and examined with an electron microscope. In negative controls, the primary antibody was replaced by phosphate-buffered saline or equimolar concentrations of non-immune rabbit IgG or an irrelevant primary antibody.

Analysis of Protein Phosphorylation—Phosphorylated proteins were purified from HaCaT cell lysates containing 2 mM EDTA, 25 μM chymostatin, 10 μM antipain, 15 μM leupeptin, and 20 μM pepstatin (all from Sigma) using the PhosphoProtein purification kit (Qiagen), following the manufacturer's instructions. For dephosphorylation, the lysates were digested with 800 units of lambda phosphatase (New England Biolabs) for 45 min at room temperature. As negative controls, a lysate containing enzyme and 10 mM activated orthovanadate, and a lysate without enzyme but with ortho-vanadate, were used. The samples were analyzed by SDS-PAGE followed by immunoblotting. Scanning densitometry of band intensities was performed using the Gel-Pro Express 4.0 software (Media Cybernetics Inc.).

For kinase inhibition experiments, the following inhibitors were used: 0.5, 1, and 2 μM casein kinase I inhibitor D4476; 100 and 150 μM casein kinase II (CK2) inhibitor 4,5,6,7-tetrabromo-2-azabenzimidazole (TBB); and 75, 100 and 150 μM protein kinase C inhibitor bisindolylamide III (all from Calbiochem). The inhibitors were dissolved in Me_2SO and added to subconfluent HaCaT cells for 2 h at 37 °C. Control cells received an equal volume of Me_2SO. Subsequently, the cells were lysed and analyzed by SDS-PAGE and immunoblotting.

Diagnosis of the Kindler Syndrome—Peripheral blood and skin samples (from non-sun-exposed skin areas) of three patients with Kindler syndrome and of age-matched control persons were obtained after informed consent and used for mutation detection, indirect immunofluorescence (IIF) staining, and cell culture. The mutation screening was performed as described elsewhere (9, 14, 15).

RESULTS

Antibody Production and Kindlin-1 Expression—Antibodies were raised against two prokaryotic recombinant fragments spanning the C terminus and one polypeptide corresponding to the N-terminal part of kindlin-1 (Fig. 1*A*). Antibody specificity was tested on lysates of COS-7 cells transiently transfected with a His-tagged full-length *KIND1* cDNA construct. Affinity-purified antibodies against kindlin-1 and antibodies against the His tag recognized a unique 78-kDa band in transfected COS-7 cells (Fig. 1*B*). In contrast, the antibodies did not react with untransfected COS-7 cells (Fig. 1*B*), which constitutively express kindlin-2 (6). The size of the polypeptide band corresponds to the molecular mass of 77.4 kDa predicted for kindlin-1 on the basis of its cDNA sequence.

The antibodies were next used to detect authentic kindlin-1 in human cells. Lysates of primary keratinocytes, HaCaT cells, and skin squamous cell carcinoma cells produced a 74-kDa/78-kDa double band in immunoblots (Fig. 1*C*). In contrast, keratinocytes of KS patients carrying kindlin-1 null mutations did not yield a signal with the antibodies (Fig. 1*C*). Interestingly, two other major cell types in human skin, epidermal melanocytes and dermal fibroblasts, produced no signal with the antibodies (Fig. 1*C*), indicating that kindlin-1 is a keratinocyte-specific protein in the skin.

In vivo, kindlin-1 is localized along the dermal-epidermal junction zone (DEJZ) in a linear pattern (Fig. 2*A*), while in KS skin there was a lack of immunofluorescence staining with kindlin-1 antibodies (Fig. 2*B*). Immunoelectron microscopy demonstrated that kindlin-1 is located in a polarized manner at the basal aspect of keratinocytes facing the basement mem-

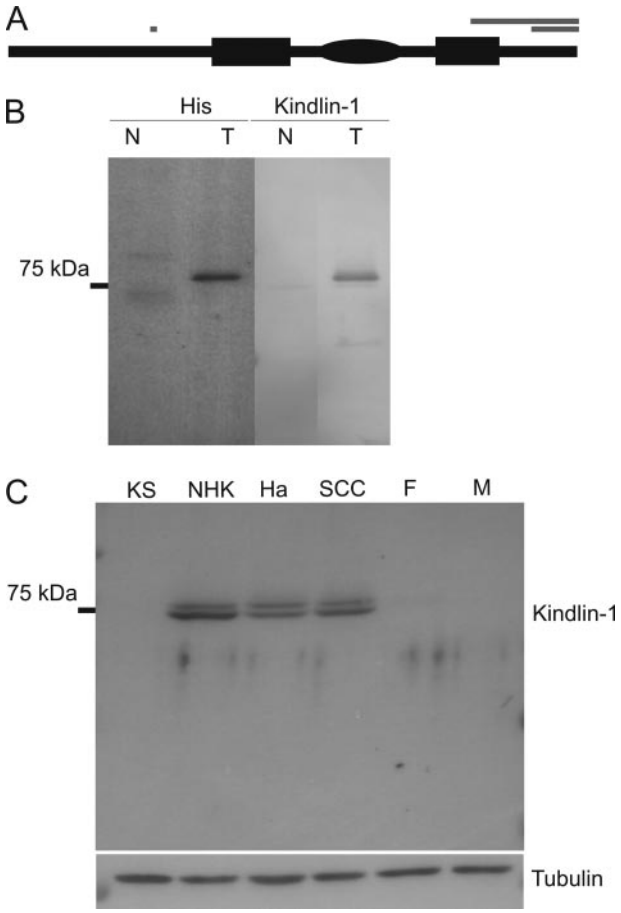

FIGURE 1. **Structure and expression of kindlin-1.** *A*, a schematic representation of kindlin-1, which is predicted to contain 677 amino acids and have a calculated molecular mass of 77.4 kDa. Kindlins have a conserved bipartite FERM domain (*rectangles*: amino acids 242–343 and 515–570) and a PH domain (ellipse: amino acids 370–475). *Gray bars* represent the recombinant glutathione *S*-transferase-kindlin-1 fragments and the polypeptide, which were used for antibody production. *B*, His-tagged kindlin-1 was expressed in COS-7 cells, which do not constitutively express kindlin-1. With both anti-His and anti-kindlin-1 antibodies, a 78-kDa band corresponding to the predicted size of authentic kindlin-1 was observed in transfected cells (*lanes T*). In untransfected cells, no staining was observed (*lanes N*). *C*, immunoblotting of cell lysates with kindlin-1 antibodies (*upper panel*) disclosed a 74-kDa/78-kDa doublet in normal human primary keratinocytes (*NHK*), HaCaT cells (*Ha*), and squamous cell carcinoma cells (*SCC*). In contrast, no signal was obtained in KS keratinocytes carrying *KIND-1* null mutations, dermal fibroblasts (*F*), or melanocytes (*M*). The *lower panel* shows an immunoblot with anti-tubulin antibodies as a loading control.

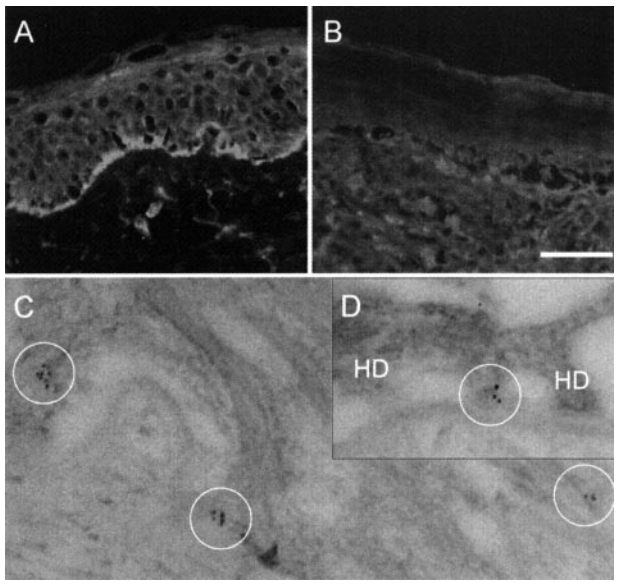

FIGURE 2. **Kindlin-1 is located at the dermal-epidermal junction.** *A*, IIF staining of normal human skin with kindlin-1 antibodies shows a linear pattern of kindlin-1 at the DEJZ. *B*, in KS skin there was a lack of IIF staining with the same antibodies. *Bar* = 50 μm. *C*, immunoelectron microscopy of normal human skin with anti-kindlin-1 antibodies revealed gold particles (*circled* in *white*) within basal keratinocytes, close to the cell membrane facing the dermal-epidermal junction. *D*, higher magnification shows that the gold particles are localized in areas between the hemidesmosomes (*HD*).

brane. The gold particles were found intracellularly, close to the plasma membrane and distributed between the hemidesmosomes (Fig. 2, *C* and *D*).

Kindlin-1 Is Phosphorylated—To explain the nature of the 74-kDa/78-kDa double band in immunoblots, both glycosylation and phosphorylation of kindlin-1 were investigated. Deglycosylation with *N*-glycosidase F did not change migration of kindlin-1 on SDS-PAGE (data not shown). However, *in silico* analysis of the amino acid sequence predicted five threonine, two tyrosine and 14 serine phosphorylation sites (Fig. 3*A*). Purification of phosphorylated proteins from HaCaT cell lysates demonstrated that the 78-kDa kindlin-1 band is phosphorylated (Fig. 3*B*). Dephosphorylation with lambda protein phosphatase led to a significant reduction of the intensity of the 78 kDa band and to an increase of the 74-kDa band (Fig. 3*C*), thus demonstrating that the latter is the unphosphorylated form. Addition of the specific CK2 inhibitor TBB to cell cultures abolished the 78 kDa form of kindlin-1 (Fig. 3*D*), but the casein kinase I inhibitor D4476 and the protein kinase C inhibitor bisindolylamide III had no influence on phosphorylation of kindlin-1 (data not shown). These experiments demonstrate that kindlin-1 is a substrate for CK2 and, consequently, that phosphorylation is likely to be involved in the regulation of kindlin-1 function.

Genetic Model: Kindlin-1 Deficiency in Kindler Syndrome—To investigate the function of kindlin-1, skin and cells of three individuals with Kindler syndrome were analyzed. Patient 1, a 6-year-old girl was homozygous for the *KIND1* mutation c.676insC, leading to a frameshift from codon 226 and to a premature termination codon 25 codons downstream. Patient 2, a female of 7-years of age, was compound heterozygous for the mutation c.910G>T, p.E304X, and for a genomic deletion starting in intron 9 and ending in intron 11, designated g.70250_74168del (15). Patient 3, a 40-year-old man, was homozygous for p.E304X (14). The clinical phenotype included pigment anomalies and extensive skin atrophy, particularly on dorsal hands, giving them a wrinkled prematurely aged appearance, more pronounced in the oldest individual (Fig. 4*A*).

In all cases the mutations caused premature termination codons and led to complete absence of kindlin-1 in the skin (Fig. 2*B*) and, notably, to several secondary aberrations. Kindlin-1-deficient epidermis was severely atrophic, with only five to six cell layers (Fig. 4*B*), and exhibited almost no reactivity with the proliferation marker Ki67, in contrast to age-matched control skin (Fig. 4, *C* and *D*), indicating that absence of kindlin-1 leads to decreased keratinocyte proliferation. The intensity of keratin 5, a marker of the intermediate filament system in proliferating

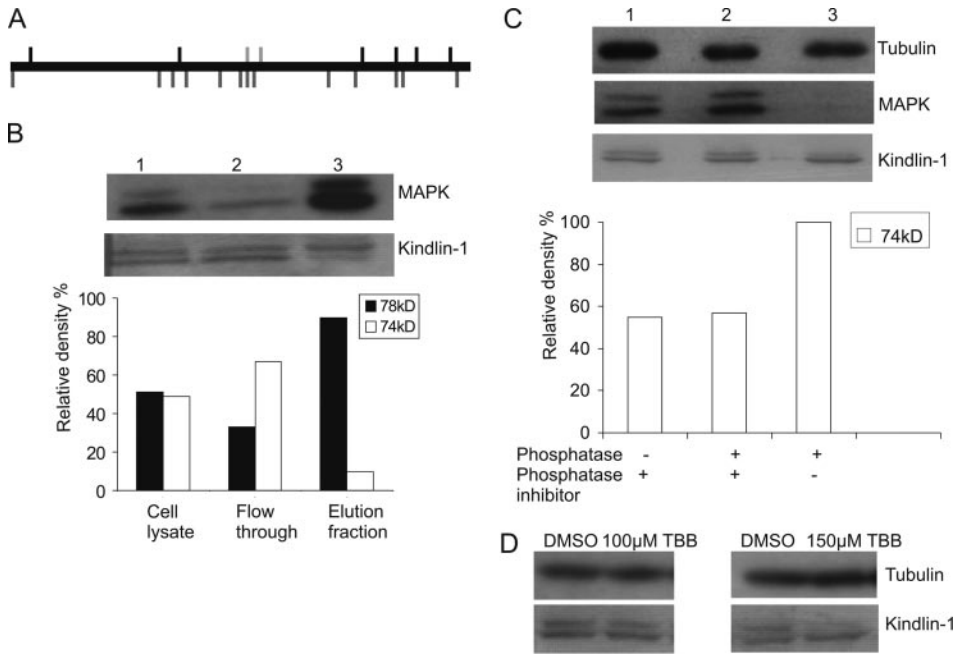

FIGURE 3. **Kindlin-1 is phosphorylated.** *A*, a schematic representation of putative phosphorylation sites in kindlin-1: *dark gray*, casein kinase II; *light gray*, tyrosin kinase; *black*, protein kinase C phosphorylation sites. *B*, phosphorylated proteins were isolated from HaCaT cell extracts using a phosphoprotein affinity column. *Lane 1*, HaCaT cell lysate used as the starting material. *Lane 2*, the unbound flow-through fraction. *Lane 3*, the elution fraction. As a control, in the *upper panel*, a blot with antibodies to phosphorylated MAPK is shown; the strong signal for the phosphorylated MAPK in the elution fraction confirms the isolation of phosphorylated proteins. The *lower panel* shows an immunoblot with kindlin-1 antibodies. Note that the 74-kDa/78-kDa kindlin-1 double band is present in the starting cell lysate and in the flow-through fraction but that the upper 78-kDa band is strongly enriched in the elution fraction, indicating that it is the phosphorylated form of kindlin-1. The *graph* shows the relative intensities of the two kindlin-1 bands. The starting material exhibits approximately equal intensities of both bands, the flow-through has more of the 74 kDa form and, in the affinity-purified fraction, the intensity of the 78-kDa band is increased 8-fold. *C*, HaCaT cell lysates were treated with lambda protein phosphatase in the presence (+) and absence (−) of the phosphatase inhibitor activated orthovanadate and immunoblotted with antibodies to kindlin-1 (*lower panel*), phosphorylated MAPK (*middle panel*), and tubulin (as a loading control, *upper panel*). Dephosphorylation occurred in the presence of the enzyme without vanadate (*lane 3*), as demonstrated by the absence of the signal for phosphorylated MAPK. In the same lane, the phosphorylated form of kindlin-1 is significantly reduced, while the lower 74-kDa band is increased in intensity, suggesting that this band represented the dephosphorylated form of kindlin-1. The *graph* shows the relative intensity of the 74-kDa band. *D*, 100 and 150 μM CK2 inhibitor TBB in Me_2SO was added to HaCaT cell cultures for 2 h. Control cells received an equal volume of Me_2SO. Cell lysates were analyzed by immunoblotting with kindlin-1 antibodies and as a loading control with tubulin antibodies. Note that TBB abolished the 78-kDa form of kindlin-1.

epidermal keratinocytes, was substantially lower in kindlin-1 deficient skin, correlating with the Ki67 signal. In particular, only the basal layer of keratinocytes was stained with antibodies against keratin 5, whereas in normal control skin two or three suprabasal cell layers were positive. In contrast, epidermal differentiation was similar in KS and control skin, as assessed by keratin 10 and involucrin staining (Fig. 4, *E–J*). The uppermost dermis contained numerous keratin 5-positive single cells (Fig. 4*E*), and the TUNEL assay revealed several apoptotic cells (Fig. 4, *K* and *L*).

Furthermore, kindlin-1 deficiency perturbed positioning of transmembrane components in basal keratinocytes. Instead of a preferential localization at the basal plasma membrane in control cells, collagen XVII was equally distributed all around the basal keratinocytes, also at the apical plasma membrane and in the cytoplasm, implicating loss of polarization (Fig. 5, *A* and *B*). Integrin α6 (Fig. 5, *C*, *D*, *G*, and *H*) and tetraspanin CD151 (data not shown), which are targeted to the ventral surface of basal keratinocytes in control skin, were strongly reduced along some DEJZ stretches, while in others the deposition seemed increased. In addition, integrin α6 was also found at the lateral and apical cell membranes in KS skin, colocalizing with α3 integrin (Fig. 5, *C–H*).

Taken together, the data show that kindlin-1 is required for keratinocyte proliferation and the polarization of transmembrane components in basal cells but not for the differentiation of epidermal keratinocytes. The clinical and immunohistochemical observations demonstrate that lack of kindlin-1 is associated with diminished proliferation, perturbed polarization, and with weak adhesion of the epidermis to the dermis.

Kindlin-1-negative Cells Have Aberrant Shape, Proliferation, Adhesion, and Migration—The aberrant features of KS keratinocytes in the epidermis were analyzed further *in vitro*. Instead of the polygonal shape and the presence of a polarized lamellipodium typical of NHK, kindlin-1-deficient keratinocytes had two or more narrow leading edges oriented in different directions (Fig. 6*A*). Approximately 40% of KS keratinocytes exhibited a bipolar, tripolar, or multipolar shape, in contrast to only 3% of normal keratinocytes. Determination of the surface area of single cells indicated that KS cells are in average significantly smaller than normal human keratinocytes (KS: 669 ± 310 μm^2; NHK: 876 ± 395 μm^2; $p < 0.0001$). However, size variability of each cell type is similar as shown by statistical distribution for the two cell populations (Fig. 6*B*).

The proliferation rate of cultivated KS cells was drastically reduced, with only one round of cell division between days 3 and 9, in contrast to normal keratinocytes, which divided three times (Fig. 6*C*). Apoptosis enzyme-linked immunosorbent assay revealed no difference between KS and normal cells (data not shown). Further functional tests revealed that the behavior of KS keratinocytes *in vitro* was significantly altered. Their adhesion to fibronectin and laminin 332 was about 44 and 61%, respectively, less than normal cells (Fig. 6*D*). In an *in vitro* wound closure assay, NHK closed the wounded area in 8 h, while in KS cell cultures the wound area was not yet filled after 12 h (Fig. 7*A*). Recording of single cell motility by video-microscopy revealed that migration of kindlin-1-deficient cells was significantly altered. Their migration trajectories tended to be random (mean index: 0.39 ± 0.19), in contrast to the directed migration typical of normal keratinocytes (mean index: 0.59 ± 0.24). The velocity of KS cells (1.50 ± 0.34 μm/min) was

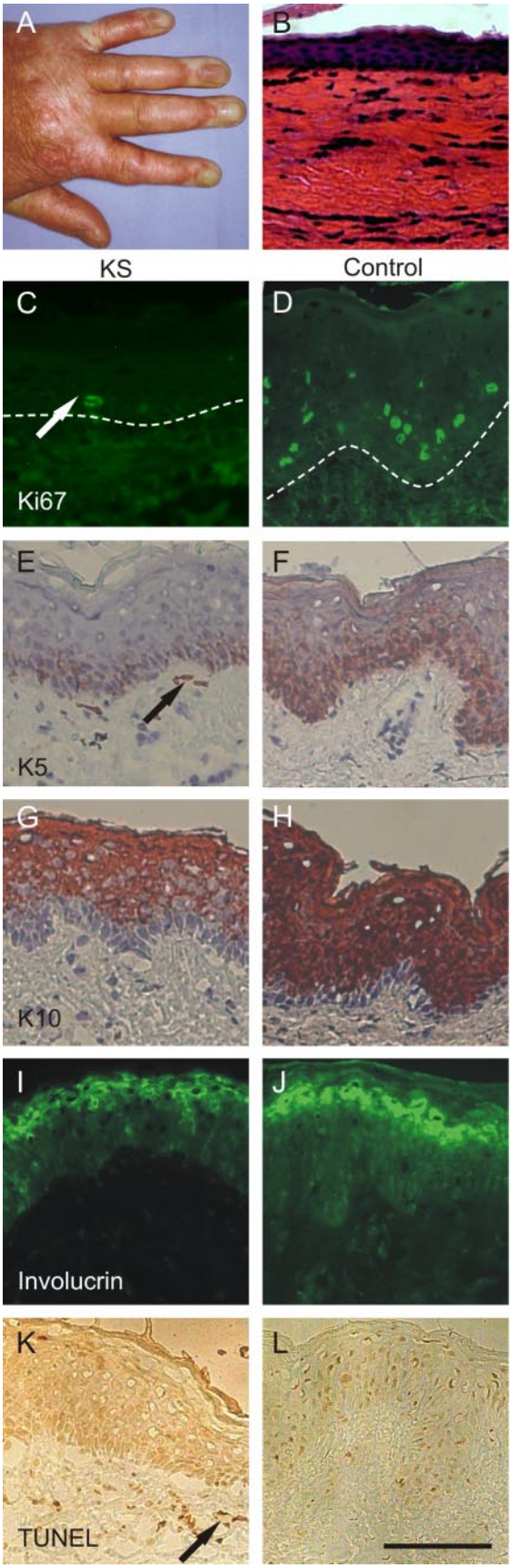

FIGURE 4. **Kindlin-1 deficiency leads to epidermal abnormalities *in vivo*.** *A*, clinical phenotype of patient 3, with skin atrophy, wrinkling, and hyperpigmentation. *B*, hematoxylin-eosin staining of a skin specimen of patient 3 shows pronounced atrophy of the epidermis and dermal fibrosis. *C*, IIF with Ki67 antibodies shows only few positive signals (*white arrow*) in the skin of patient 1. *D*, Ki67 staining of control skin. *E*, immunohistochemical staining of keratin 5 shows a very low signal in kindlin-1-negative skin. In the upper dermis, keratin 5-positive cells are found (*black arrow*). *F*, keratin 5 staining of control skin. *G*, immunohistochemical staining disclosed keratin 10 in the suprabasal layers in kindlin-1-negative skin. *H*, keratin 10 staining of control skin. *I*, IIF with involucrin antibodies shows staining of the granular layer in kindlin-1-negative skin. *J*, IIF with involucrin antibodies shows staining of the granular layer in control skin. *K*, apoptotic cells were detected by the TUNEL assay in the upper dermis of KS skin. *L*, TUNEL assay of control skin remained negative. *Bar* = 50 μm, all panels have the same magnification.

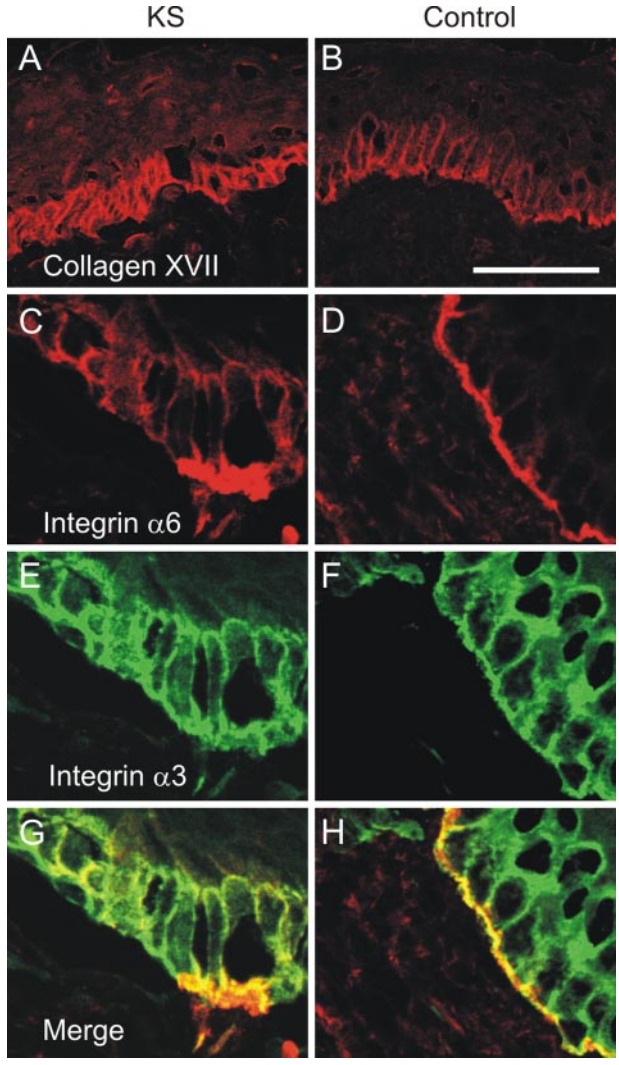

FIGURE 5. **Defective polarization of basal keratinocytes in kindlin-1-deficient skin.** *A*, collagen XVII was abnormally distributed in kindlin-1-deficient skin, diffusely in the cytoplasma and associated with the entire cell membrane of the basal keratinocytes, while in the control skin (*B*), it was concentrated at the DEJZ. *C*, skin sections of patient 2 stained with antibodies to α6 integrin and α3 integrin (*E*); *G*, the merge of α6 and α3 integrin staining. *D*, control skin stained with antibodies against α6 integrin; *F*, α3 integrin; *H*, the merge of α6 and α3 integrin stainings. While α6 and α3 integrin co-localize linearly at the DEJZ in control skin, they co-localize at the cytoplasmic membrane of the basal keratinocytes in KS skin (*G*, *H*).

slightly, nevertheless significantly, lower than that of normal keratinocytes (1.87 $\pm$ 0.44 μm/min) (Fig. 7*B*).

In addition, on video-microscopy recordings, KS cells were changing shape to a greater extent than NHK. These changes were analyzed in more details by measuring, in successive

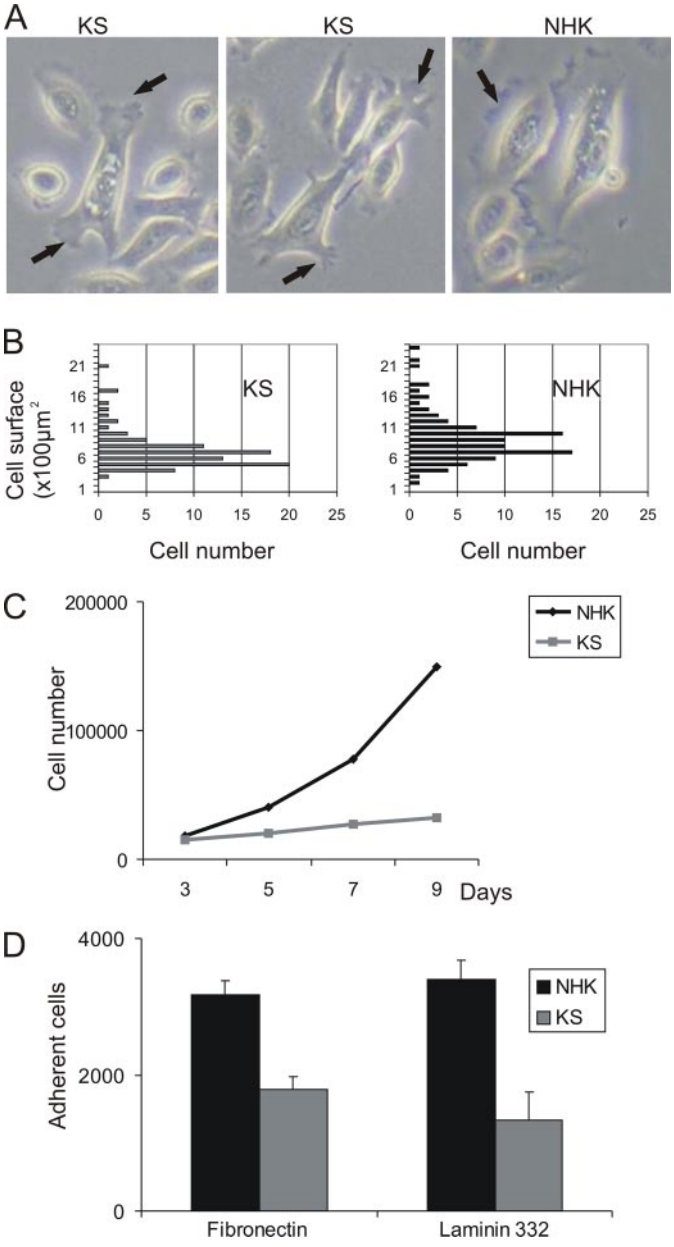

FIGURE 6. **Kindlin-1 deficiency causes aberrant cell shape, altered proliferation, and adhesion.** *A*, keratinocytes in culture were photographed by phase contrast microscopy. In the *left* and *middle panels*, kindlin-1-deficient keratinocytes show altered multipolar morphology with multiple leading edges (*black arrows*). In contrast, NHK in the *right panel* displayed a polarized lamellipodium (*arrow*). *B*, the surface of KS ($n = 88$) and normal human keratinocytes ($n = 100$) was measured using the software ImageJ. The cell area in μm^2 was grouped as follows: 0–100, 100–200, etc. The surface of 85% of kindlin-1-deficient KS was 300–800 μm^2, while in 75% of NHK the surface area ranged between 500 and 1000 μm^2. This indicated that KS cells are in average significantly smaller than NHK (KS: 669 ± 310 μm^2; NHK: 876 ± 395 μm^2; $p < 0.0001$). *C*, to analyze proliferation, 10^4 KS keratinocytes and NHK were seeded on plastic, cultivated for 3, 5, 7, or 9 days, and then washed, trypsinized, and counted. The growth curve shows that KS cells proliferated significantly slower than normal cells, only about one cell division in 6 days. The experiments were done in duplicate. *D*, to assess cell adhesion, equal amounts of NHK and KS keratinocytes were plated for 1 h on surfaces coated with fibronectin or laminin 332, washed, trypsinized, and counted. The adhesion of KS cells to fibronectin and laminin 332 was about 44 and 61%, respectively, less than normal cells.

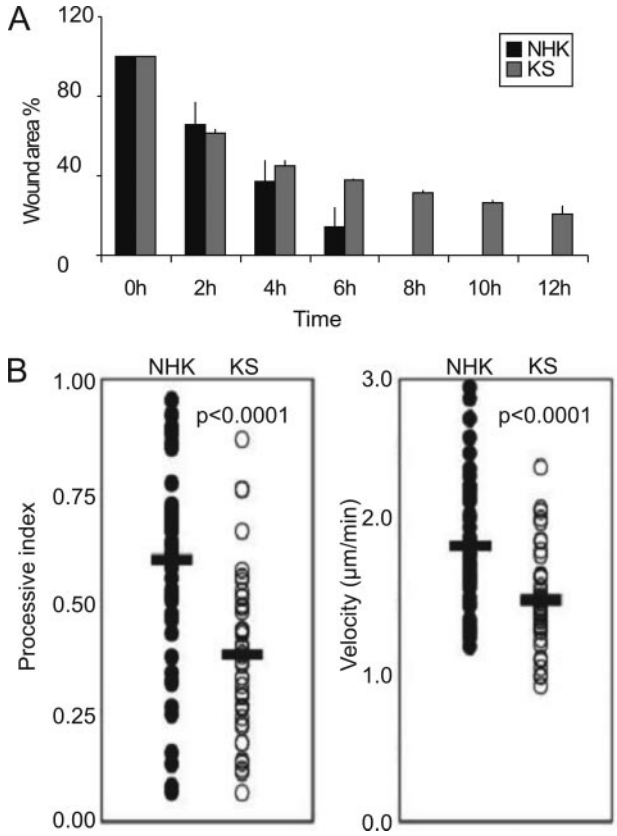

FIGURE 7. **Altered motility of KS keratinocytes.** *A*, cell migration was analyzed with an *in vitro* wound closure assay. NHK closed the wounded area in 6–8 h, but KS keratinocytes had not yet closed the wound after 12 h. *B*, cell motility was recorded for 3 h by time-lapse video microscopy. The migration routes of single cells were analyzed on QuickTime movies and used to determine individual processive indexes (*left panel*) and the velocity (*right panel*) for 45 NHK (*black circles*) and 41 KS keratinocytes (*white circles*). The mean processive index and velocity are marked with the *black bars*; for both parameters, the statistical difference between NHK and KS cells is highly significant ($p < 0.0001$).

frames of the movies, the cell area involved in retraction and protrusion of the plasma membrane (Fig. 8*A*). Quantitative measurements revealed that changes in cell shape affected 17.2 ± 4.2% of the total surface of KS cells, as compared with only 6.4 ± 1.9% in NHK (Fig. 8*B*). Moreover, while protrusion and retraction often occurred at the same time on opposite sides of the cell in normal keratinocytes, as reported previously (16), protrusion and retraction of the cell membrane were anarchic for KS cells (Fig. 8*A*), which agrees with their non-polarized, close to random migration (Fig. 7*B*).

DISCUSSION

In this study we characterized authentic kindlin-1 in human skin and primary keratinocytes and explored its functions using genetic, recombinant expression, protein and immunochemical, and cell biological approaches. Kindlin-1 emerged a few years ago, when mutations in its gene, *KIND-1*, were disclosed as the cause of KS (1, 8), a puzzling clinical disorder resembling both blistering diseases and poikilodermatic syndromes (8). Some molecular features of kindlin-1 were then discerned, *e.g.* its transforming growth factor-β responsiveness or its binding to β1 integrin (7) and association with focal contacts (vinculin) and actin (1, 7). Therefore, the KS is the first human skin fragility disorder caused by deficiency of a β1 integrin-associated focal adhesion protein. However, very little was known about native kindlin-1 or its physiological functions.

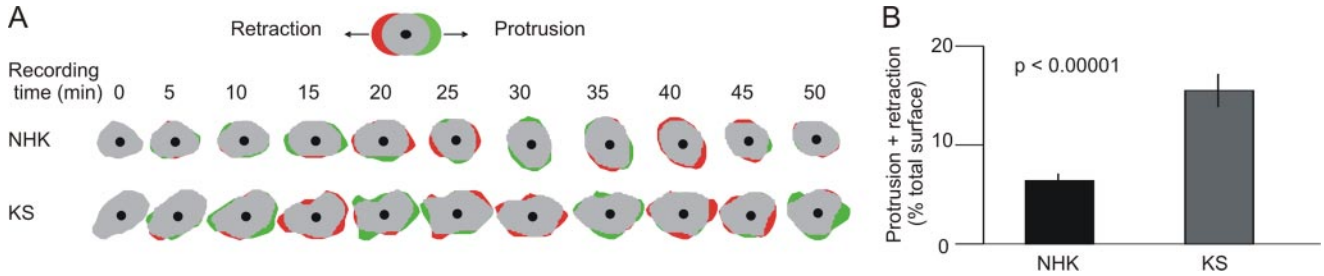

FIGURE 8. **Plasma membrane movements in NHK and KS keratinocytes.** *A*, movements of the cell membrane of NHK and KS keratinocytes were recorded with time-lapse video microscopy and converted to QuickTime movies. Cell shape changes were determined by measuring in successive frames (1 frame/5 min) the plasma membrane areas involved in protrusion (*green*) and retraction (*red*) for single cells. Examples of time-lapse sequences (50 min) are shown for one NHK and one KS keratinocyte. *B*, quantification of plasma membrane areas undergoing changes (protrusion and retraction added) for NHK (*black column*) and KS (*gray column*) keratinocytes. The *graph* shows mean and standard deviation calculated from measurements applied to five cells in each population (24 measurements/cell). The difference between control and KS keratinocytes is highly significant ($p < 0.00001$).

First we generated antibodies that specifically react with human kindlin-1, but not with the related family member kindlin-2, and showed that kindlin-1 is an intracellular, keratinocyte-specific protein. It exists in two forms, phosphorylated and non-phosphorylated, with apparent sizes of 78 and 74 kDa, respectively, corresponding well to the calculated molecular mass of 77,437 Da for the precursor polypeptide.

Similarly to many cytoskeleton associated proteins, CK2 was implicated in the phosphorylation process, because TBB, a cell-permeable, highly selectively ATP/GTP competitive inhibitor of CK2 (17), efficiently diminished phosphorylation of kindlin-1. CK2 is a ubiquitously expressed serine/threonine kinase in eukaryotic cells, which influences a wide variety of cellular processes like differentiation, proliferation, cell cycle control, and cellular response to stress, such as UV radiation (18). It is involved in the regulation of cell morphology, namely in the maintenance of cell shape and polarity, and in the regulation of the actin cytoskeleton through interactions with actin capping proteins (19). More than 300 substrates have been identified for CK2, it phosphorylates membrane-associated and cytoskeletal proteins including akrin, spectrin, dystrophin, calmodulin, troponin, myosin, and caldesmon (for review, see Ref. 19). Even if kindlins are not typical FERM proteins, because their FERM domain is interrupted and not placed N-terminally, it is notable that phosphorylated FERM proteins are selectively found in cell-surface associated structures. For these reasons we predict that phosphorylation represents a regulatory mechanism for the activity of kindlin-1, although the significance of phosphorylation *in vivo* still remains elusive.

Novel information on kindlin-1 functions was obtained through analysis of phenotypic consequences of *KIND-1* mutations. It was known that the tissue architecture and the epidermal compartment appear abnormal in KS skin, with reduplications of the lamina densa, lysis of the extracellular matrix in the upper dermis, and focal clefting in the lamina lucida (reviewed in Ref 8). Accordingly, in the skin of the younger KS patients 1 and 2 of this study, many areas showed extensive tissue separation beneath or in the basal keratinocyte layer, and collagen IV, $\alpha6\beta4$ integrin, and laminins 332 and 511 were present in a discontinuous pattern, contributing to the adhesion defect of basal keratinocytes. Kindlin-1-deficient basal keratinocytes exhibited abnormal polarity *in vivo* and *in vitro*. The epidermis contained rounded or flattened basal keratinocytes, which did not form a palisade-like architecture, and the intracellular distribution of collagen XVII and $\alpha6$ integrin indicated loss of polarization. In culture, KS keratinocytes were small, had abnormal shape with multiple leading edges, and adhered poorly to fibronectin and laminin 332, indicating that the presence of these extracellular matrix components could not rescue the phenotype. Intriguingly, the epidermal detachment and the disorganization of the basement membrane zone in KS skin are similar to that seen in the skin of conditional $\alpha3$ and $\beta1$ integrin null mice (20–23) suggesting that kindlin-1 and $\alpha3\beta1$ integrin are functionally related in determining cell polarity and adhesion.

In the skin of the 40-year-old patient 3, the epidermis was severely atrophic. Phenotype analyses provided evidence for impaired epidermal proliferation but showed that terminal differentiation is spatially and temporally maintained in KS skin. Kindlin-1-deficient epidermis was thinner, consisting of a flattened basal cell layer, a few layers of spinous cells expressing keratin 10, a granular layer, and a stratum corneum with normal appearance. The cellular abnormalities concerned mainly the basal layer, with disorganized keratinocytes apparently loosing their proper architecture, polarization, and the boundary to the dermis. The cells exhibited minimal expression of the proliferation marker Ki67, and staining of keratin 5, a cytoskeletal hallmark of the proliferating basal layer of the epidermis, was substantially reduced as compared with controls. These observations suggest that kindlin-1 has a physiological function in cell proliferation, a prediction supported by the slow dividing potential of KS keratinocytes in culture. Interestingly, deficiency of a kindlin-1 ligand, $\beta1$ integrin, decreased proliferation of basal keratinocytes by about 70% in a mouse model (22). Similarly to $\beta1$ integrin deficiency, absence of kindlin-1 may impair cell cycle progression (23).

Keratin 5-positive cells were observed in the upper dermis in the three individuals with KS, but no evidence was found for the extensive intraepidermal apoptosis reported in some KS cases (24). Kindlin-1 deficiency was also not associated with enhanced apoptosis of cultured keratinocytes. Thus, environmental factors and time are likely to play a role in induction of the apoptotic process *in vivo*. In $\beta1$ integrin-deficient mouse skin, apoptosis was not a feature (22), suggesting that different pathways are activated in the two deficiencies, at least in part. In KS skin, the proliferation defect, together with loss of basal keratinocytes through apoptosis, explains the profound atrophy.

Directed migration of cells is essential in development, maintenance of multicellular organisms, and in regenerative processes, such as wound healing. The common attribute of moving cells is the lamellipodium, a broad flat-like structure that contains a polarized network of actin filaments. The process of moving is dependent on integrin-mediated cell adhesion and polarized changes of the cytoskeleton and is controlled by Rho GTPases (25). Kindlin-1-deficient keratinocytes migrated slower and in an undirected manner, a behavior accompanied by abnormal cell morphology, loss of polarization, and presence of two or more leading edges.

Taken together, the structural and functional defects observed in KS keratinocytes seem to be interconnected. Although we do not yet fully understand the physiological functions of kindlin-1 or the molecular disease mechanism in KS, the present study revealed intriguing novel aspects. Through its binding to the cytoplasmic domain of β1 integrin (7), kindlin-1 is likely to participate in a number of integrin mediated processes, such as cell attachment to the extracellular matrix and stabilization of the integrin-associated platforms allowing force transmission between the extracellular matrix and the cytoskeleton, the integrity of which is needed for cell polarity, cell migration, cell cycle progression, gene expression, and survival (25).

Acknowledgments—We thank Margit Schubert, Käthe Thoma, Bernhard Kremer, and Monika Pesch for expert technical assistance and Dr. Gianlucca Tadini for sending skin and blood samples of patient 2.

REFERENCES

1. Siegel, D. H., Ashton, G. H., Penagos, H. G., Lee, J. V., Feiler, H. S., Wilhelmsen, K. C., South, A. P., Smith, F. J., Prescott, A. R., Wessagowit, V., Oyama, N., Akiyama, M., Al Aboud, D., Al Aboud, K., Al Githami, A., Al Hawsawi, K., Al Ismaily, A., Al Suwaid, R., Atherton, D. J., Caputo, R., Fine, J. D., Frieden, I. J., Fuchs, E., Haber, R. M., Harada, T., Kitajima, Y., Mallory, S. B., Ogawa, H., Sahin, S., Shimizu, H., Suga, Y., Tadini, G., Tsuchiya, K., Wiebe, C. B., Wojnarowska, F., Zaghloul, A. B., Hamada, T., Mallipeddi, R., Eady, R. A., McLean, W. H., McGrath, J. A., and Epstein, E. H. (2003) *Am. J. Hum. Genet.* **73,** 174–187
2. Rogalski, T. M., Mullen, G. P., Gilbert, M. M., Williams, B. D., and Moerman, D. G. (2000) *J. Cell Biol.* **150,** 253–264
3. Bretscher, A., Edwards, K., and Fehon, R. G. (2002) *Nat. Rev. Mol. Cell. Biol.* **3,** 586–599
4. Balla, T. (2005) *J. Cell Sci.* **118,** 2093–2104
5. Gkretsi, V., Zhang, Y., Tu, Y., Chen, K., Stolz, D. B., Yang, Y., Watkins, S. C., and Wu, C. (2005) *J. Cell Sci.* **118,** 697–710
6. Tu, Y., Wu, S., Shi, X., Chen, K., and Wu, C. (2003) *Cell* **113,** 37–47
7. Kloeker, S., Major, M. B., Calderwood, D. A., Ginsberg, M. H., Jones, D. A., and Beckerle, M. C. (2004) *J. Biol. Chem.* **279,** 6824–6833
8. White, S. J., and McLean, W. H. (2005) *J. Dermatol. Sci.* **38,** 169–175
9. Jobard, F., Bouadjar, B., Caux, F., Hadj-Rabia, S., Has, C., Matsuda, F., Weissenbach, J., Lathrop, M., Prud'homme, J. F., and Fischer, J. (2003) *Hum. Mol. Genet.* **12,** 925–935
10. Raghavan, S., Vaezi, A., and Fuchs, E. (2003) *Dev. Cell* **5,** 415–427
11. Tasanen, K., Tunggal, L., Chometon, G., Bruckner-Tuderman, L., and Aumailley, M. (2004) *Am. J. Pathol.* **164,** 2027–2038
12. Schacke, H., Schumann, H., Hammami-Hauasli, N., Raghunath, M., and Bruckner-Tuderman, L. (1998) *J. Biol. Chem.* **273,** 25937–25943
13. Tasanen, K., Eble, J. A., Aumailley, M., Schumann, H., Baetge, J., Tu, H., Bruckner, P., and Bruckner-Tuderman, L. (2000) *J. Biol. Chem.* **275,** 3093–3099
14. Has, C., and Bruckner-Tuderman, L. (2004) *J. Invest Dermatol.* **122,** 84–86
15. Has, C., Wessagowit, V., Pascucci, M., Baer, C., Didona, B., Wilhelm, C., Pedicelli, C., Locatelli, A., Kohlhase, J., Ashton, G. H., Tadini, G., Zambruno, G., Bruckner-Tuderman, L., McGrath, J. A., and Castiglia, D. (2006) *J. Invest Dermatol.* **126,** 1776–1783
16. Frank, D. E., and Carter, W. G. (2004) *J. Cell Sci.* **117,** 1351–1363
17. Ruzzene, M., Penzo, D., and Pinna, L. A. (2002) *Biochem. J.* **364,** 41–47
18. Bibby, A. C., and Litchfield, D. W. (2005) *Int. J. Biol. Sci.* **1,** 67–79
19. Canton, D. A., and Litchfield, D. W. (2006) *Cell. Signal.* **18,** 267–275
20. DiPersio, C. M., Hodivala-Dilke, K. M., Jaenisch, R., Kreidberg, J. A., and Hynes, R. O. (1997) *J. Cell Biol.* **137,** 729–742
21. Raghavan, S., Bauer, C., Mundschau, G., Li, Q., and Fuchs, E. (2000) *J. Cell Biol.* **150,** 1149–1160
22. Brakebusch, C., Grose, R., Quondamatteo, F., Ramirez, A., Jorcano, J. L., Pirro, A., Svensson, M., Herken, R., Sasaki, T., Timpl, R., Werner, S., and Fassler, R. (2000) *EMBO J.* **19,** 3990–4003
23. Brakebusch, C., and Fassler, R. (2005) *Cancer Metastasis Rev.* **24,** 403–411
24. Lanschuetzer, C. M., Muss, W. H., Emberger, M., Pohla-Gubo, G., Klausegger, A., Bauer, J. W., and Hintner, H. (2004) *Hum. Genet.* **115,** 175
25. Hynes, R. O. (2002) *Cell* **110,** 673–687